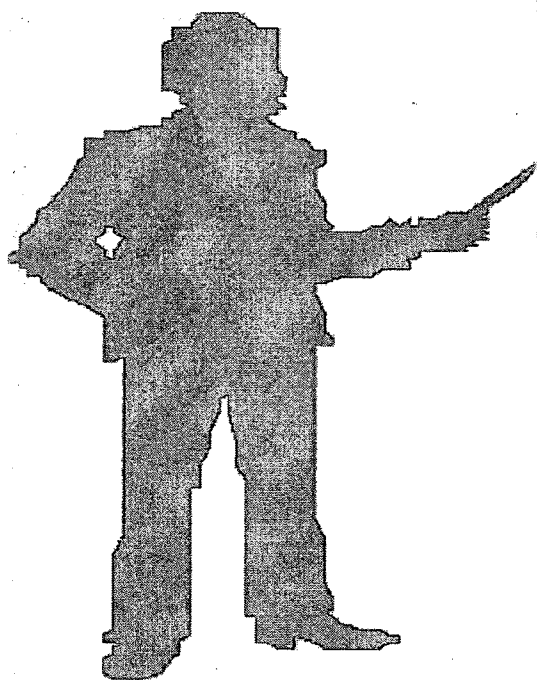


Chapter VII



**Docetaxel Loaded
Polymersomes:
Development and
Characterization
In Vitro and *In Vivo***

Tije et al., 2003). Therefore, investigation of alternative doses form of docetaxel without polysorbate 80 is now theme of scientist and increasing number of papers has been reported on the alternative formulation of docetaxel such as docetaxel conjugation (Esmaeili et al., 2009; Xie et al., 2009), nanoparticles (Esmaeili et al., 2008; Feng et al., 2009; Chan et al., 2009; Xu et al., 2009), liposomes (Immordino et al., 2003), polymeric nanoparticles (Hwang et al., 2008), micelles (Elsabahy et al., 2007; Liu et al., 2008), and prodrug (Du et al., 2007; Huynh et al., 2009) have been investigated.

In this chapter, we encapsulated docetaxel (DOC) in PBLG₂₃-*b*-HYA₁₀ polymersomes and characterized *in vitro* and *in vivo*. Pharmacokinetic and biodistribution profile was investigated on normal rabbits and EAT tumor bearing BalB/c mice respectively.

7.2. Material

Docetaxel trihydrate was given as a gift sample by Sun Pharmaceutical Ltd. INDIA. Polysorbate 80 and Ethanol were purchased from Sigma Aldrich, INDIA.

7.3. Formulation of docetaxel loaded polymersomes (PolyDOC) and docetaxel solution (DS)

Docetaxel (DOC) loading was performed at different feed weight ratio of DOC: PBLG₂₃-*b*-HYA₁₀ by nanoprecipitation. DOC and block copolymer was dissolved in warm DMSO, then tris buffer (10 mM, 154mM ionic strength with pH = 7.4) was injected at 18 mL/h (with a 5 ml syringe) or 36 mL/h (with a 10 ml syringe) in DMSO (block copolymer concentration = 0.5 wt %) with continuously stirring at 55°C for final concentration of copolymer 1mg/mL (0.1 wt %). The unloaded DOC and DMSO were removed by dialysis (MWCO = 2000g/mol, 6 Spectra/Por® membrane) against tris buffer (10 mM, 154mM ionic strength with pH = 7.4) (Hwang et al., 2008; Gao et al., 2008). Samples were dialyzed against 1000 times of outside medium, with 2 changes of this medium in 8h followed by 24h. Loading content of DOC was determined after extraction of DOC from lyophilized PolyDOC in ethanol (100%) through vortex for 20 minutes and then left for 10 minutes at RT. Sample was filtered (0.45µm, Nylon) and subjected for UV measurement at $\lambda_{\max} = 230$ nm. Quantification was performed from the

calibration curve of DOC in ethanol. Samples were characterized by light scattering (DLS) and by microscopy (FF-TEM and AFM).

$$\text{Loading Content} = \frac{\text{Drug amount in loaded vesicle}}{\text{Amount of vesicle}} \times 100$$

$$\text{Loading Efficiency} = \frac{\text{Drug Amount in Loaded Vesicle}}{\text{Initial Amount of Drug}} \times 100$$

We prepared docetaxel solution (DS) for *in vivo* comparative study with PolyDOC. DOC (5mg) was solubilized in polysorbate 80 (1040mg or 1mL) followed by dilution with 10% ethanol in PBS (pH = 7.4) for final 0.25mg/mL concentration of DOC for ^{99m}Tc labeling, pharmacokinetic and biodistribution study. Final concentration of polysorbate 80 and ethanol will be 5% and 10% respectively in 0.25mg/mL DS. This formulation was further diluted with PBS for concentration 100µg/mL to 10µg/mL for hemolytic activity. This formulation was stable for more than experimental time (48h). Fresh sample was prepared before each experiment.

7.4. *In vitro* release studies

We have investigated the DOC release profile at pH 7.4 tris buffer and pH 5.5 acetate buffer. The required amount of drug loaded vesicles (3-4mL) were poured in dialysis tube [Spectra/Por® Float-A-Lyzer™, Dialysis Tubes, MWCO: 25000 g/mol, diameter: 10mm, Volume: 10mL). Dialysis tube was introduced in a 50 mL measuring cylinder in vertical position containing 50 mL of tris buffer pH = 7.4 or acetate buffer pH 5.5 with 2 % v/v ethanol to enhanced the solubility of release free DOC and avoid aggregation of free DOC. Whole assembly was kept at 37°C ± 2 and covered by the parafilm to avoid the evaporation. 2 mL of sample was withdrawn at each sampling time and replace with same volume of fresh respective buffers (containing 2 % v/v pure ethanol) to maintain the required sink conditions. Quantification was done by the calibration curve of DOC in respective buffers solution.

7.5. Stability studies

PolyDOC prepared at different feed weight ratios (DOC/copolymer) were investigated for stability at room temperature (RT) and at 4°C temperature. PolyDOC formulations

were divided into two batches, one batch kept at RT and the other one at 4°C. Loading content was determined as per above mentioned procedure and hydrodynamic radius was determined as per mention in chapter III and IV. Before analysis, 4°C samples have been vortexes for one minute.

7.6. Lyophilization process

PolyDOC formulations were investigated for lyophilization process. PolyDOC samples were frozen with liquid nitrogen in 10 mL vials and then lyophilized (CHRIST, ALPHA 1-2 LD plus, BIOBLOCK SCIENTIFIC). After 48h, samples were removed from the lyophilizer, reconstituted with the required amount of tris buffer and vortexed for 10min followed by sonication (2-10min). Loading content was determined as per above mentioned procedure and hydrodynamic radius was determined as per mention in chapter III and IV of samples before and after the lyophilization.

7.7. *In vitro* cytotoxicity studies on MCF-7 and U87

The cytotoxic effect of free DOC in 0.2% v/v DMSO (Free DOC) and PolyDOC on the cells was determined by the MTT (3-(4,5-dimethylthiazol-2-yl)-2,5-diphenyl tetrazolium bromide) assay. Cells were seeded in a 96-well plate (5000/well) containing 200µL cell culture media. Different concentration (100nM, 50nM, 30nM, 10nM, and 1nM equivalent to free DOC) of PolyDOC and free DOC were incubated with cells for 24, 48, and 72h. Subsequently after end time points, cells were incubated with 10% MTT solution (5mg/mL in PBS) in incubator at 37°C for 2h. The cells were lysed and the formazan crystals dissolved using DMSO (150µL) at the end of incubation. The absorbance was noted at 570 nm using 630 nm as reference wavelength on multiwell plate reader (Biotek instruments, USA). Control sample was treated as incubation without free DOC, and PolyDOC. Absorbance was directly related to % cell viability and control cell viability was considered 100% cell viability at each respective time points:

$$\% \text{ cell viability} = \left(\frac{N_t}{N_u} \right) \times 100, \text{ where } N_t \text{ and } N_u \text{ are the number of surviving cells in the}$$

treated groups with free DOC and PolyDOC in the untreated group respectively.

7.8. ^{99m}Tc labeling of DS and PolyDOC

The Radiolabeling of DS and PolyDOC were performed as per published procedure with slightly modification (Liu et al., 1997, Reddy et al., 2005 and Meléndez-Alafort et al., 2006). A 25 μL stannous chloride (2 mg/mL in 0.1 M Acetic Acid) was added in 100 μL of saline containing pertechnetate ($^{99m}\text{TcO}_4^-$) (3mCi; obtained by solvent extraction method from molybdenum). The resulting solution was incubated for 10 min at room temperature (RT), after adjusting the pH to 6.5 with the help of 0.5 M NaHCO_3 and so called reduced technetium. PolyDOC and DS (0.25mg/mL, equivalent to free DOC) were added with reduced technetium and incubated at RT for 30 minutes. Nitrogen gas was passed to degas all the solutions prior to the mixing or incubation. Labeling efficiency and radiochemical purity (Saha 2004, Harivardhan Reddy et al., 2005, Panwar et al., 2007) was confirmed by ascending instant thin-layer chromatography using silica gel-coated fiber sheets (ITLC-SG) (Gelman Science Inc., Ann Arbor, MI, USA) and 100% acetone was used as mobile phase. ITLC-SG was carried out by running a sample of 2-3 μL on a 10 cm strips using acetone as mobile phases. The solvent front was allowed to reach up to a height of about 8 cm from the origin. The strip was cut into two halves (Top and Bottom) and the radioactivity in each half was determined by a well type gamma ray spectrometer (Type GRS23C, Electronics Corporation of India Limited, India). The free pertechnetate ($R_f = 0.9-1.0$) migrates to the top portion of the ITLC-SG strip, leaving the labeled complex at the bottom. Furthermore, radiochemical purity and labeled efficiency was adjusted by subtracting the migrated activity of unwanted radio colloids in pyridine: acetic acid: water (3:5:1.5). The radio colloids remained at the bottom of the strip, while both the free pertechnetate and the labeled complex migrated with the solvent front. We also checked particle size after radiolabeling of PolyDOC.

$$\text{Free } ^{99m}\text{Tc} \% = \frac{T}{T+B} \times 100\%$$

$$\% \text{ Labeling} = (100 - \% \text{ free } ^{99m}\text{Tc})$$

$$\% \text{ Purity} = (100 - \% \text{ radio colloids})$$

Where T is the counts at top and B is the counts at bottom.

7.9. Transchelation of complexes

In order to check the strength of binding of ^{99m}Tc with the PolyDOC and DS, 0.5 ml of the labeled preparation was challenged against various concentrations (10, 30 50 and 100 mM) of Diethylenetriaminepentaacetic acid (DTPA) (Mishra et al., 2002, Reddy et al., 2005) and incubated for 1 h at 37°C . The effect of DTPA on labeling efficiency was measured on ITLC-SG using acetone as the mobile phase, which allowed the separation of free pertechnetate and DTPA-complex ($R_f = 0.8-1.0$) from the ^{99m}Tc -DS and ^{99m}Tc -PolyDOC which remained at the point of application ($R_f = 0$).

7.10. *In vitro* and *in vivo* stability of radiolabel compounds

In vitro stability of the radio labelled formulations was monitored in freshly collected human serum and Phosphate buffered saline (PBS) (pH =7.4) at 37°C for 48h at 1:1 ratio (50% v/v). At several time points, post incubation (1, 4, 24 and 48h), samples were analyzed for the radio labeling efficiency using ITLC-SG as described above. In addition we determined dilution stability of radio labelled compounds. To determine the stability of radio labeled complexes after dilution, 100 μl of complex was diluted to a ratio 1:100 in saline and incubated for 24h at 37°C . The radio labeling efficiency of complex was analyzed by ITLC-SG as described above.

In vivo stability of radio labelled compound was investigated in normal, healthy, female New Zealand rabbits weighing 2.3–2.9 kg. All animal studies were carried out under the guidelines compiled by CPCSEA (Committee for the Purpose of Control and Supervision of Experiments on Animals, Ministry of Culture, Govt. of India) and all the study protocols were approved by institutional animal ethics committee. ^{99m}Tc (0.5 mCi) (0.5mL injected volume containing 25 μg /0.1mL equivalent concentration of DOC) labeled formulations was injected in rabbits through the dorsal ear vein. The blood was withdrawn through the vein of other ear at different periodic intervals and spotted on the ITLC-SG strips and ITLC-SG carried out as described previously to estimate the possible separation of free ^{99m}Tc .

7.11. Pharmacokinetic study of ^{99m}Tc -PolyDOC and ^{99m}Tc -DS

Pharmacokinetic study was performed in normal, healthy, female New Zealand rabbits (n = 3 per group) weighing 2.0-2.5 kg. Animals were injected with 0.5mCi ^{99m}Tc -labeled PolyDOC and DS (0.5mL injected volume containing 25 μg /0.1mL equivalent concentration of DOC) through the dorsal ear vein. The blood samples were withdrawn through the vein of the other ear at different periodic intervals in pre-weighed tubes. The weight of the blood withdrawn at each sampling point was recorded and the radioactivity measured using a well-type γ -ray spectrometer (Type CRS 23C, Electronic Corporation of India Ltd.) along with an injection standard. The activity present in total blood was calculated by considering 7.3% of total body weight as total blood weight (Wu et al., 1981, Arulsuda et al., 2004, Agashe et al., 2007). Data were adjusted with *in vivo* stability data of their respective formulation.

7.12. Hemolysis effect

The hemolysis test was conducted as described by Shuai et al., 2004 with slightly modification. Fresh human blood (healthy 30 year old, type B positive male with normal blood chemistry) collected in heparin tubes (LABTECH Disposables, INDIA) from pathology lab. In brief, blood was washed three times with PBS and red blood cells (RBCs) collected by centrifugation at 2800 rpm for 5 min. The washing step was repeated in order to remove debris and serum protein. The PolyDOC and DS at different concentrations varying from 10 to 100 $\mu\text{g}/\text{mL}$ were used for experiment. Typically, 100 μl of the erythrocyte suspension were added to 900 μl of formulations. The samples were incubated for 60 min at 37 $^{\circ}\text{C}$ in incubator with intermittent shaking. The release of hemoglobin was measured by UV-Vis analysis of the supernatant at 540 nm after centrifugation at 3000rpm for 60 minutes. Erythrocytes incubated with saline and distilled water served as negative (0%) and positive controls (100%), respectively and all hemolysis data points are presented as the percentage of the complete hemolysis. The results of the hemoglobin assay was adjusted by subtraction of the absorbance of the no-blood control (i.e., sample containing all assay components except the blood is substituted by PBS) (Marina et al., 2008). The % hemolysis rate (%HR) was calculated from the following equation.

$$\% HR = \frac{A_t - A_{nc}}{A_{pc} - A_{nc}} \times 100$$

Where A_t , A_{nc} , and A_{pc} are the absorbance of the tested sample, the negative control, and the positive control, respectively. The experiments were run in triplicate.

7.13. Biodistribution study of ^{99m}Tc -PolyDOC and ^{99m}Tc -DS

Female BalB/c mice (aged 2 months), weighing between 20 and 24 g were selected for the study. EAT tumor developed in mice as per mention in chapter VI. Randomly animals were divided into two groups containing three animals per group. All animals were fasted overnight before the experiment but allowed free access to water. Each of the mice received an injected dose of 100 μCi of the ^{99m}Tc -DS and ^{99m}Tc -PolyDOC (equivalent to DOC 2mg/kg body weight) was administered by the tail vein of each mouse. Injected volume in mice was adjusted as required dose but not more than 10g/0.1mL of mice weight.

The mice were humanely sacrificed at 1, 4, and 24hours post injection. The blood was collected by the inferior vena cava and subjected to reperfusion with saline to remove blood components from the blood vessels presence in tissues. Subsequently different organs like heart, lung, liver, kidney, spleen, stomach, intestine, and tissues like muscles and tumor were dissected. The organs and tissues were collected in pre-weighed tubes after washing them with normal saline and drying. Organs were weighed and radioactivity corresponding to them was measured using well-type γ -scintillation counter along with an injection standard. The percentage of injected dose per gram of tissue (%ID/g) and the liver-to-blood and tumor-to-muscle ratios were calculated.

7.14. Statistical analysis

All data expressed as means \pm standard deviation (S.D.) are representative of at least three or six different experiments. Difference between two groups was evaluated using Student's t-test. A "P" value less than 0.05 was considered statistically significant difference.

7.15. Results and Discussion

7.15.1 Docetaxel loaded polymersomes (PolyDOC)

Docetaxel trihydrate (DOC) (Mw=861.94), (Figure 7.1) is an anti-mitotic chemotherapeutic agent and taxane class derivate. DOC targets microtubules, components of the cell cytoskeleton and essential to the production of the mitotic spindle. Treatment with taxanes results in stabilization of the microtubules leading to cell cycle arrest in the G2/M phase (Vaishampayan et al., 1999). It is poorly water soluble drug therefore used as hydrophobic model drug to investigate potentiality of novel PBLG₂₃-b-HYA₁₀ polymersomes for chemotherapy. DOC calibration curves was prepared from freshly prepare stock solution of DOC (50 μ g/mL) in tris buffer (10 mM, 154mM ionic strength with pH=7.4) with 10% ethanol, in acetate buffer (pH = 5.5) with 10% ethanol at $\lambda_{\max} = 230$ nm. Figure 7.2 A is calibration curves of DOC and also calibration curve of DOC was plotted (Figure 7.2B) in pure ethanol at $\lambda_{\max} = 230$ nm for further use in DOC estimation.

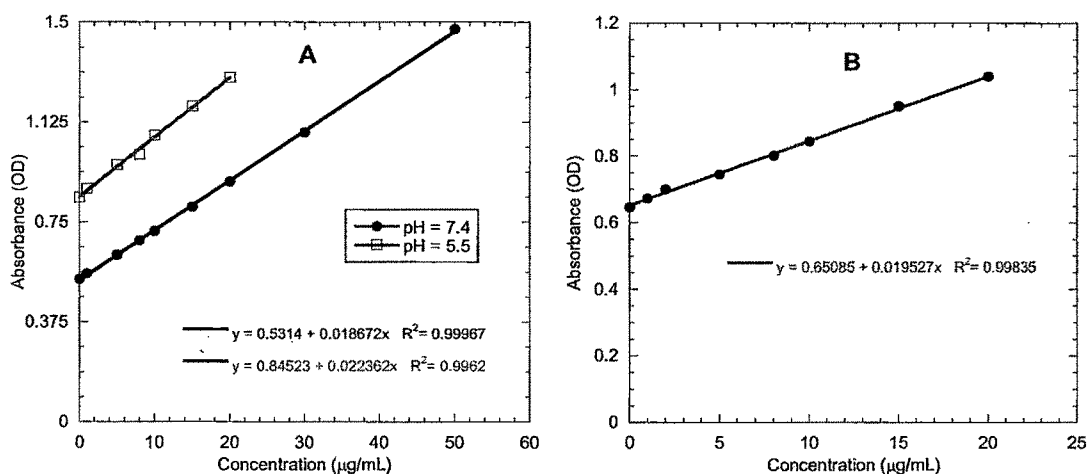


Figure 7. 2 (A) Calibration curve of DOC in tris buffer (pH = 7.4) and in acetate buffer (pH = 5.5), (B) Calibration curve of DOC in ethanol.

DOC loading was performed at different feed weight ratio (drug/copolymer) by nanoprecipitation (Table 7.1). Final DOC loading in polymersomes was 9.81 ± 0.66 % (i.e. $\sim 100\mu$ g of drug/mg of polymersomes) with encapsulation efficiency of about 49%. The hydrodynamic radius of PolyDOC was determined to be $R_H = 135 \pm 10$ nm (Figure 7.3 and Table 7.2) by dynamic light scattering (DLS) after sonication of preformed

PolyDOC for 10 min using ultra sonic processor (130 watt, 20 kHz, Vibra Cell, 75186) at 60% amplitude, at program, pulse 2 second on and 1 second off. Total energy consumption was 0004216 Joules with 001 to 020 watts for 10 minutes.

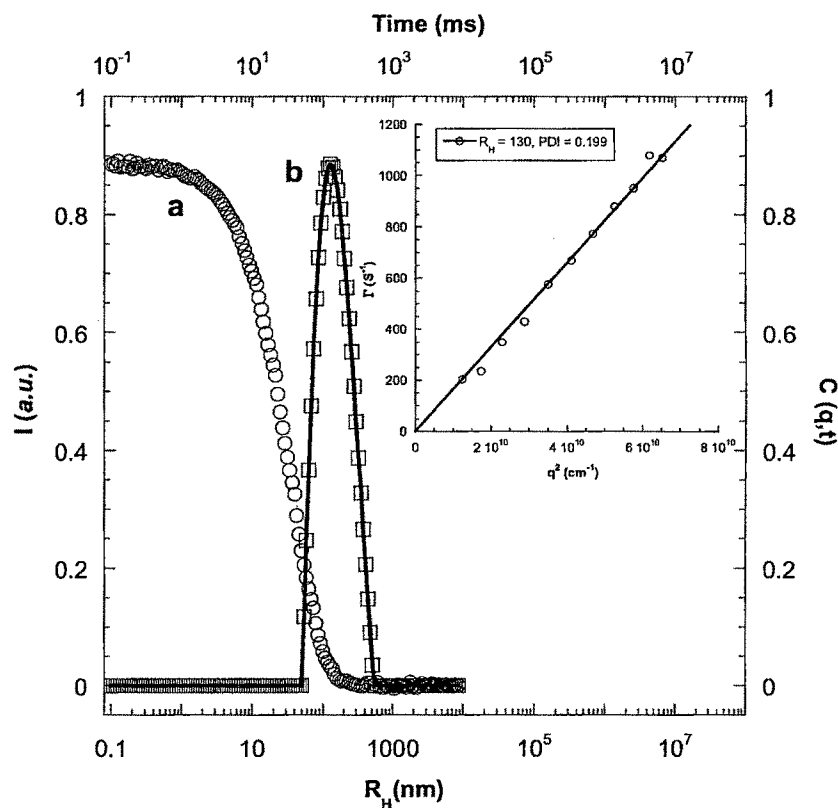


Figure 7.3 DLS autocorrelation function of the PBLG₂₃-*b*-HYA₁₀ polymersomes (a) and their time relaxation distribution at 90° scattering angle (b). The inset shows the decay rate Γ dependency to the square scattering vector q^2 .

Table 7.1 Drug loading content and efficacy of PolyDOC*

S.No	Feed Weight Ratio DOC/Copolymer	Loading Content	Loading Efficiency
1.	0.05:1	1.71 ± 0.44	34.18 ± 8.85
2.	0.1:1	2.77 ± 0.27	27.68 ± 2.69
3.	0.2:1	9.81 ± 0.66	49.07 ± 3.32

*Each value is the mean ±S.D. of three experiments (n=3).

Table 7.2 DLS result of PolyDOC formulations before and after probe sonication (10 minute)

S.No.	Formulation	After Removal of Docetaxel		After Probe Sonication (10min)	
		R _H (nm)	PDI	R _H (nm)	PDI
1.	0.05:1	428	0.441	130	0.199
2.	0.1:1	459	0.309	131	0.237
3.	0.2:1	558	0.419	139	0.435

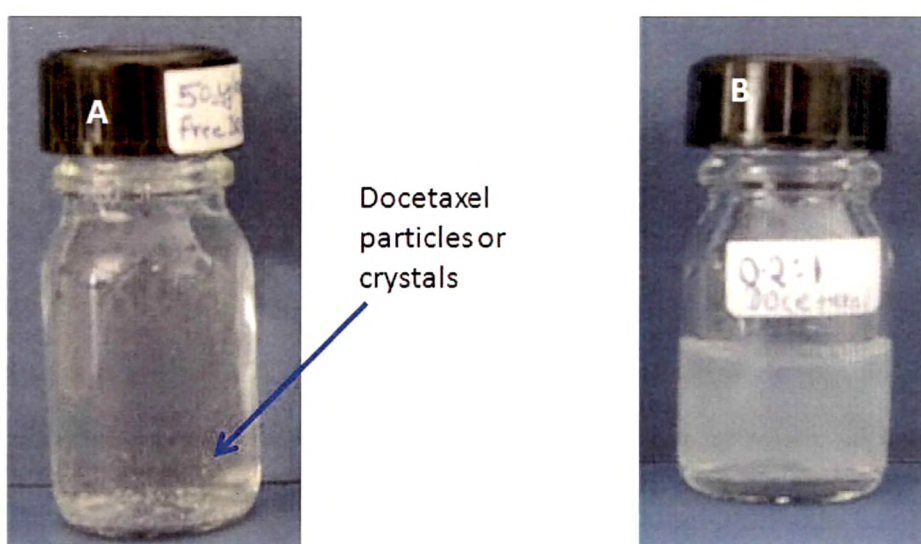


Figure: 7.4. (A) 50µg/mL of DOC in tris buffer (pH= 7.4). (B) 100µg/mL of DOC loaded PolyDOC. Arrow indicates DOC crystals and particles.

Figure 7.4 clearly indicates DOC insoluble particles or crystals at 50µg/mL in tris buffer (pH = 7.4) just after 30 minutes storage. However, no free DOC particles and no crystals were observed after encapsulation of DOC in polymersomes at the concentration of ~100µg/mL even after 5 days storage at 4⁰C. PolyDOC morphologically characterized by freeze fracture-TEM (Figure 7.5) and AFM (Figure 7.6 and 7.7) as per mention procedure in chapter III and IV and represent typical loaded polymersomes images.



Figure 7.5 FF-TEM of PolyDOC.

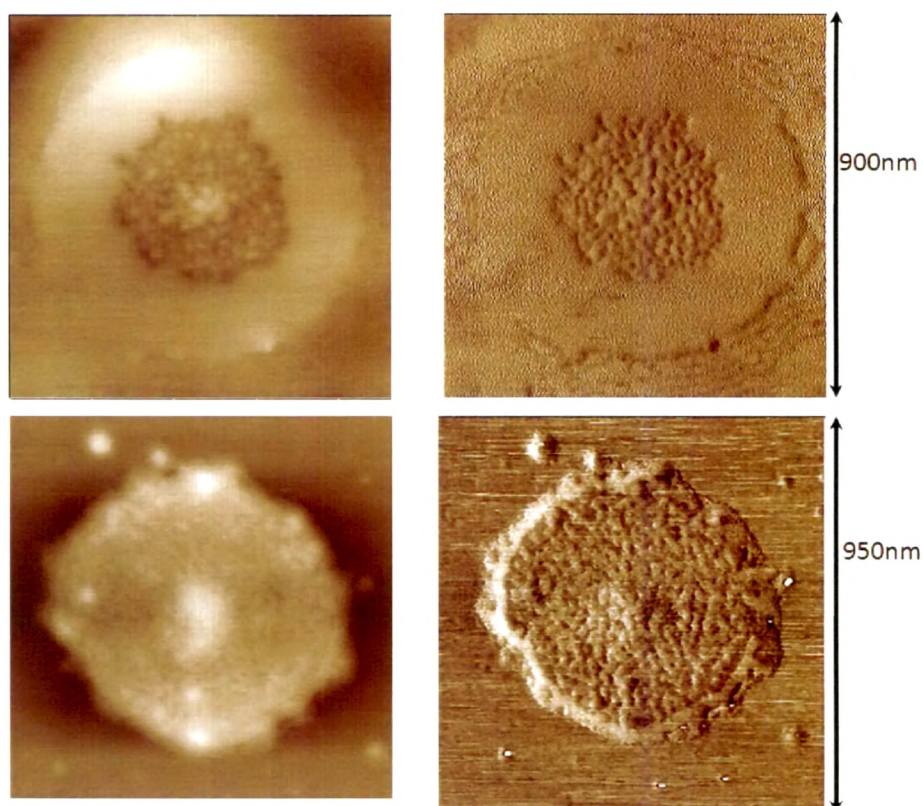


Figure 7.6 AFM analysis of PolyDOC.

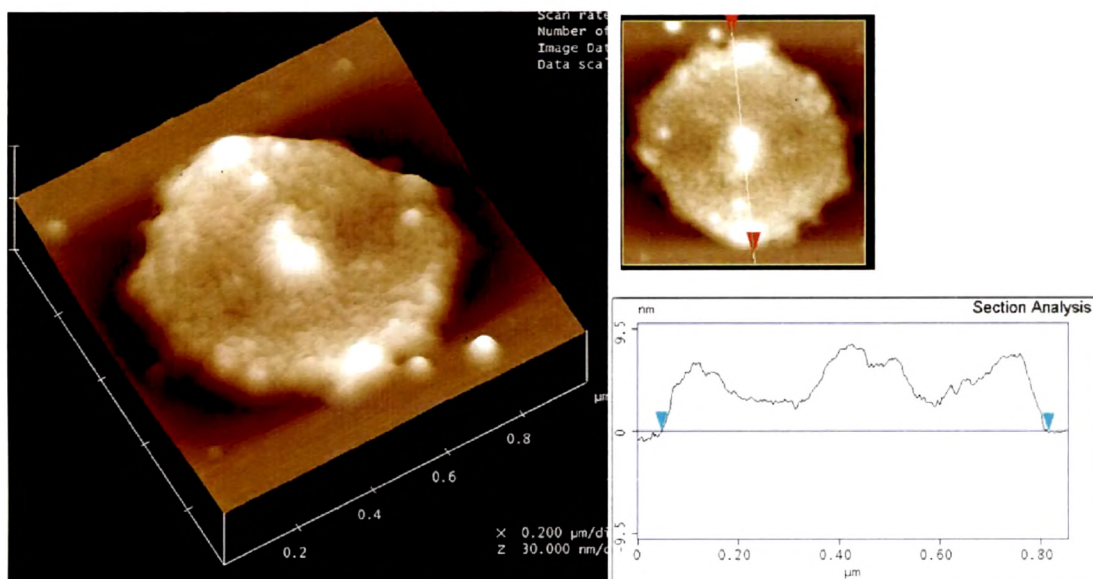


Figure 7.7 Section analysis in AFM image of selected PolyDOC.

Stability of PolyDOC formulations was examined at both RT and at 4⁰C for one month. At both storage conditions, loose aggregates were formed but they disappeared after one minute of vortexing or hand shaking without affecting hydrodynamic radius (R_H). Above than 90% DOC was recovered after storage of PolyDOC at 4⁰C. However, PolyDOC is also stable at RT except 0.2:1 batch; it shows very few particles or crystals which we considered not to be stable formulation in one month storage at RT. The stability of PolyDOC formulations was enhanced by lyophilization process (Figure 7.8).



Figure 7.8 Lyophilized PolyDOC.

As we have already discussed in chapter III, the presence of 40% wt of hyaluronan in polymersomes act as cryoprotectant in lyophilization process and protect the vesicular morphology after reconstitution in aqueous solutions. There was no significant difference in loading content before and after lyophilization storage at 4⁰C for more than six months. Full redispersion of lyophilized vesicles was achieved in tris buffer by vortexing

for 10min followed by sonication (2-10min) in order to accelerate the dispersion time and eventually eliminate the few aggregates still present in solution.

Figure 7.9 illustrate DOC release profile in the acetate buffer pH 5.5 and tris buffer pH 7.4 medium. Free DOC was completely released in 4h whereas sustain release behavior of DOC was observed in both pH after being loaded in Polymersomes. PolyDOC release more than 20% of DOC in 24h and remaining DOC released up to 10 days. Fitting of the experimental data was assessed using well known diffusion release kinetic Higuchi model ($M_t = M_\infty kt^{1/2}$), where M_t and M_∞ represent mass release at time (t) and at infinite time (∞) respectively, k is a diffusion coefficient constant and t is time for study period. We have plotted the data using the Higuchi representation (Figure 7.10), that give correlation coefficient close to 1 which indicate DOC was release by diffusion mechanism.

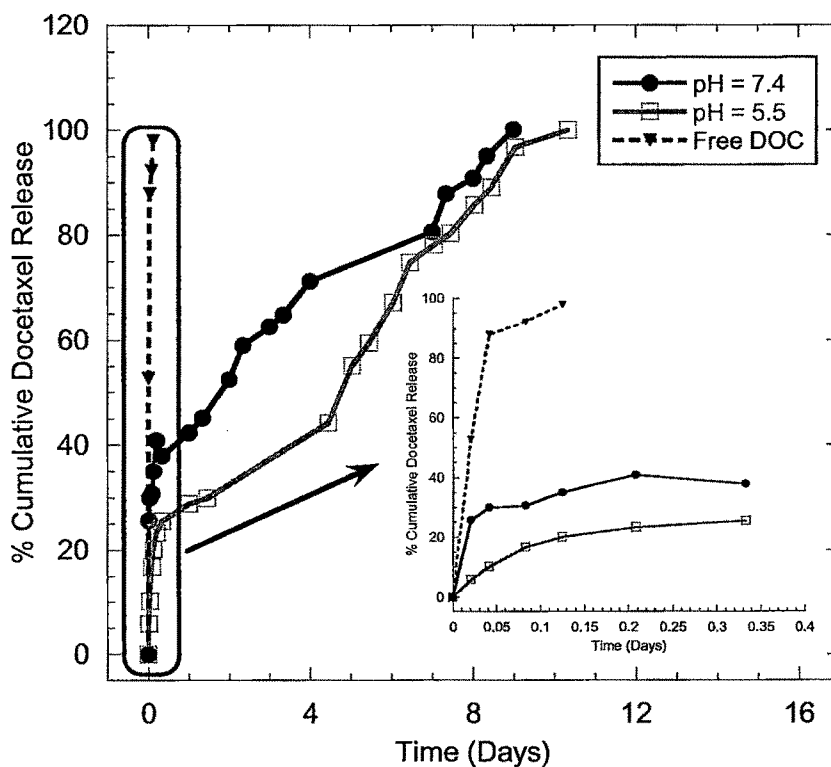


Figure 7.9 *In vitro* release patterns of free DOC and loaded DOC at pH 5.5 and 7.4.

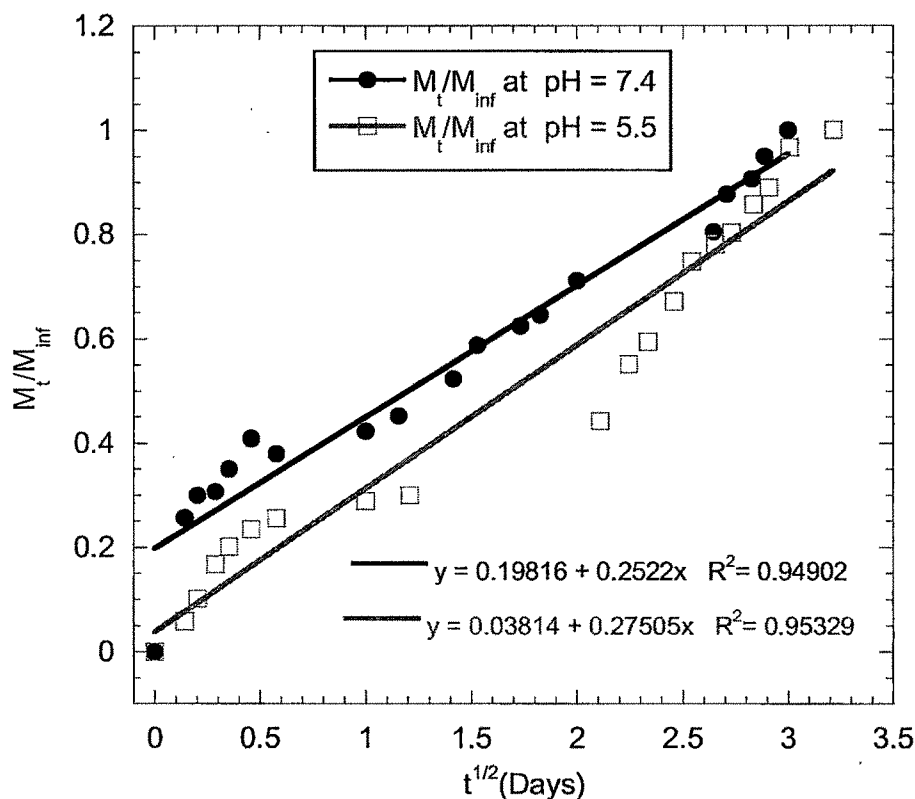


Figure 7.10 Higuchi representations of *in vitro* release profiles of PolyDOC at pH 5.5 and 7.4.

7.15.2 Cytotoxicity study

The *in vitro* cytotoxic of the free DOC, and PolyDOC was evaluated using the MCF-7 cells and U87 cells that are positive for CD44 glycoprotein receptor for hyaluronan with high expression (MCF-7) and low expression (U87). The used quantity of DMSO solvent for solubilization of free DOC was not affected viability of both cells and cell viabilities being all above 95%.

Dose response curve were plotted between different concentration of compounds and % cell viability (Figure 7.11 and 7.12). Cytotoxicity was dependent on exposure time and concentration of free DOC, and PolyDOC. Cell viability was decrease as exposure time and concentration of compounds increase in both cells. IC_{50} value was calculated from dose response curve (Figure 7.11 and 7.12) using OriginPro 7.5 software and presented in table 7.3.

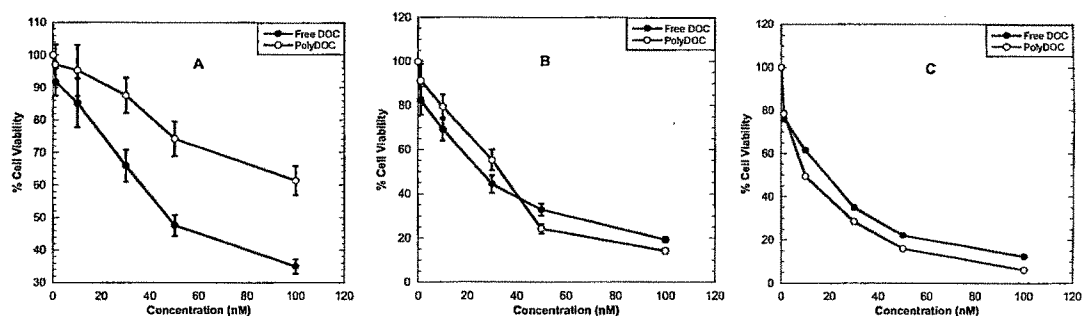


Figure 7.11 A, B and C is the % cell viability with free DOC, and PolyDOC in MCF-7 cells at 24, 48 and 72h respectively. Data represent mean \pm SD (n = 6).

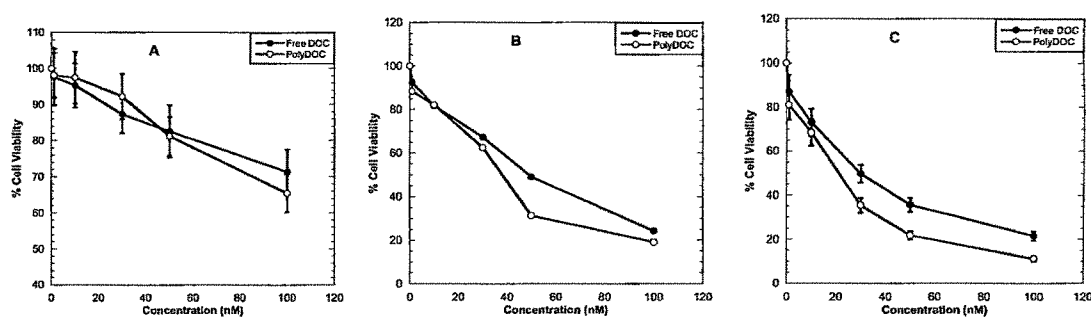


Figure 7.12 A, B and C is the % cell viability with free DOC, and PolyDOC in U87 cells at 24, 48 and 72h respectively. Data represent mean \pm SD (n = 6).

Table 7.3 *In Vitro* Cytotoxicity of PolyDOC and Free DOC (Concentration in nM), IC₅₀#

Exposure Time (h)	MCF-7		U87	
	Free DOC	PolyDOC	Free DOC	PolyDOC
24	55.29	> 100	> 100	> 100
48	25.22	31.40	50.62	38.95
72	14.07	8.43*	30.50	20.61*

#IC₅₀ inhibitory concentration of DOC producing 50% of cell growth.

*P < 0.01 vs. free DOC.

Free DOC was significant potent ($P < 0.05$) at 24h but at 72h PolyDOC was produced significant ($P < 0.01$) cytotoxicity compare to free DOC in MCF-7 cells. U87 cells express p-glycoprotein pump (Pgp) (Rittierodt and Harada 2003) therefore viability was not affected after exposure with free DOC at 24h. PolyDOC was significant ($P < 0.01$) produce cytotoxicity in both cells compare to free DOC at 72h. MCF-7 cells express high

CD44 hyaluronan receptor level (Chapter V) compare to U87 therefore PolyDOC was significantly more potent in MCF-7 cells than U87 cells in each time point.

7.15.3 ^{99m}Tc -Labeled DS and PolyDOC

Figure 7.13 represents ^{99m}Tc labeling efficiency of the compounds. All compounds were labelled with ^{99m}Tc by direct labeling method and represent more than 98% labeling efficiency together with less than 2% impurities (free $^{99m}\text{TcO}_4^-$, and radio colloids).

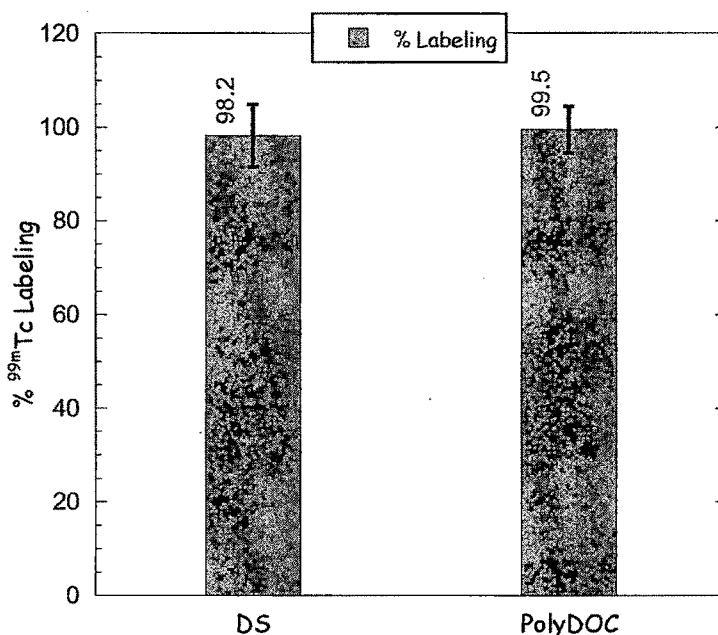


Figure 7.13 ^{99m}Tc Radiolabeling efficiency of DS and PolyDOC.

DTPA challenge was performed to determine the binding strength of ^{99m}Tc -DS and ^{99m}Tc -PolyDOC. No considerable effect was observed on labeling efficiency of the complexes even at higher concentration (100mM) of DTPA (Table 7.4) and which indicate strong and stable complex between ^{99m}Tc and Taxotere and PolyDOC.

Table 7.5, represent *in vitro* stability of the labeled formulations in PBS (pH = 7.4) and in human serum. *In vitro* stability was determined up to 48h. The data confirmed excellent stability of the labeled complexes in PBS and serum up to 48h as indicated by their labeling efficiency (Table 7.5). Labeling efficiency was found more than 95% in PBS and more than 89% in presence of serum. Labeling efficiency of ^{99m}Tc -DS and ^{99m}Tc -PolyDOC was ~90% at 100 times dilution after incubation for 24h at 37⁰C (Table

7.6). In addition, above than 88% labeling efficiency was observed *in vivo* at different time points (Table 7.7).

We have explained in chapter VI that hyaluronan contain hydroxyl and carboxyl functional group, which can coordinate with metal core and produce stable radio labeled complex (Meléndez-Alafort et al., 2006). This could be the explanation of their good stability *in vitro* and *in vivo*. Above mentioned results of *in vitro* and *in vivo* stability suggests that ^{99m}Tc radionuclide could be ideal radio tracer as markers for the *in vivo* application in our study.

Table 7.4 *In vitro* stability of ^{99m}Tc -labelled compound in presence of DTPA (n=3)

% Transchelation with DTPA		
Conc. (mM)	DS	PolyDOC
10	ND	ND
30	1.21±0.04	1.01±0.07
50	3.48±0.21	1.47±0.13
100	7.32±0.49	4.99±0.26

Table 7.5 *In vitro* stability of ^{99m}Tc -labelled compound in PBS and serum (n=3)

Post incubation time (h)	PBS		Serum	
	DS	PolyDOC	DS	PolyDOC
1	98.41±5.29	99.27±2.62	98.21±3.47	99.23±3.18
4	98.27±3.46	99.96±2.41	97.62±4.01	98.47±2.29
24	97.38±5.72	99.01±3.82	91.02±2.97	95.17±4.21
48	95.73±4.19	98.46±3.11	89.11±5.82	91.97±4.01

Table 7.6 *In vitro* stability after 100 times dilution of ^{99m}Tc -labeled compounds (n=3)

Incubation time (h)	DS	PolyDOC
0	98.11±4.79	99.28±3.41
2	96.34±3.82	98.97±3.88
5	94.29±4.63	98.04±5.35
24	88.91±5.18	91.36±2.82

Table 7.7 *In vivo* stability of ^{99m}Tc -labeled compounds (n = 3)

Sampling time (h)	DS	PolyDOC
1	97.82±4.21	99.10±3.49
4	97.45±5.37	98.12±3.71
24	90.01±3.12	92.27±4.19
48	88.21±4.18	90.31±5.72

7.15.4 Blood Clearance study of ^{99m}Tc labeled compounds

The blood clearance profile of ^{99m}Tc -PolyDOC and ^{99m}Tc -DS are shown in figure 7.14 after the IV bolus injection. All the ^{99m}Tc -labeled compounds were rapidly cleared from the blood circulation. However, there was significant difference ($P < 0.01$) in plasma profile between the injected ^{99m}Tc -PolyDOC and ^{99m}Tc -DS. PolyDOC concentration was significantly higher ($P < 0.001$) in bloodstream than that of DS at each sampling time.

Non-compartmental pharmacokinetic analysis was performed using AUC+ method in Kinetica-4.4 (InnaPhase Corp, Philadelphia, PA, USA) for IV bolus. The area under the plasma concentration-time curve (AUC^0_{∞}) was calculated by using the linear trapezoidal method. The terminal elimination rate constant (λ_z) was estimated from the slope of the terminal phase of the log plasma concentration-time points fitted by the method of least-squares, and then the terminal elimination half-life ($T_{1/2}$) was calculated as $0.693/\lambda_z$. The values of apparent volume of distribution during the terminal phase (V_z) and apparent volume of the plasma compartment (V_{ss}) were directly derived from software. The total clearance (CL) was calculated as $0.693 \cdot V_z / T_{1/2}$. All pharmacokinetic parameters are presented in Table 7.8.

The PolyDOC significantly increased ($P < 0.001$) the half-life ($T_{1/2}$; 19.90h), mean residence time (MRT; 26.86h) and area under the curve (AUC; 89.73% h/mL) of DOC in circulation, as compared with DS ($T_{1/2}$; 4.79h, MRT; 5.96h, AUC; 24.24% h/ml). These results indicate that PolyDOC can circulate for a longer time in the blood circulation system than DS.

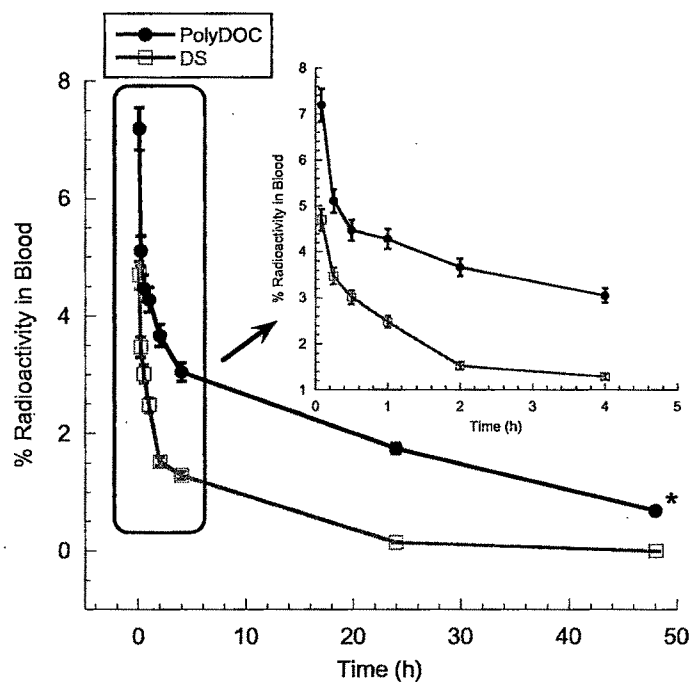


Figure 7.14 Pharmacokinetic profiles of DS, and PolyDOC after single intravenous injection in rabbit. (* $P < 0.001$ vs. DS). The data represent the mean \pm S.D (n = 3).

Table 7.8 Pharmacokinetic parameters of ^{99m}Tc -Labeled compounds in rabbits (n=3)

Pharmacokinetic Parameters	DS	PolyDOC*
C_{\max} (%)	4.69	7.19
T_{\max} (h)	0.083	0.083
AUC_{0-48} (%h/mL)	24.24	89.73
$T_{1/2}$ (h)	4.79	19.90
MRT(h)	5.966	26.86
Lz (h^{-1})	0.144	0.035
CL (%/h)	0.798	0.793
V_z (mL)	5.52	22.77
V_{ss} (mL)	4.76	21.30

* $P < 0.001$ vs. DOC

Above mention results suggest that hyaluronan stabilized polymersomes can prolong the blood circulation time of DOC after IV administration. Remarkably, presence of hydrophilic surface due to hyaluronan on the PolyDOC protected DOC from the serum proteins and prolonged its half-life as compared with those of the DS formulation. Hyaluronan has been reported as hydrophilic material for coating on liposome for enhancement of long circulating time compare to PEGylated liposome (Doxil) in healthy and tumor bearing mice (Peer and Margalit 2004).

7.15.5 Hemolysis effect of PolyDOC and DS

Hemolytic profile is presented in figure 7.15 of PolyDOC and DS at different concentration. The hemolytic activity of the PolyDOC was examined and the RBC lysis profiles were expressed as the percentage of hemoglobin released relative to the positive and negative control. PolyDOC was found to be non-hemolytic (i.e., less than 5% hemoglobin released) at all concentrations examined (10 μ g/mL to 100 μ g/mL DOC equivalent concentration). However, more than 30% hemolytic activity was observed with DS formulation (100 μ g/mL). At the same concentration, taxotere has reported more than 40% RBC lysis (Quaglia et al., 2009). Main constitute in taxotere is Tween 80, have been reported to interact with cell membrane of RBC and cause significant hemolytic activity (Cheon Lee et al., 2003). Therefore PolyDOC are apparently more hemocompatible compared to DS formulation.

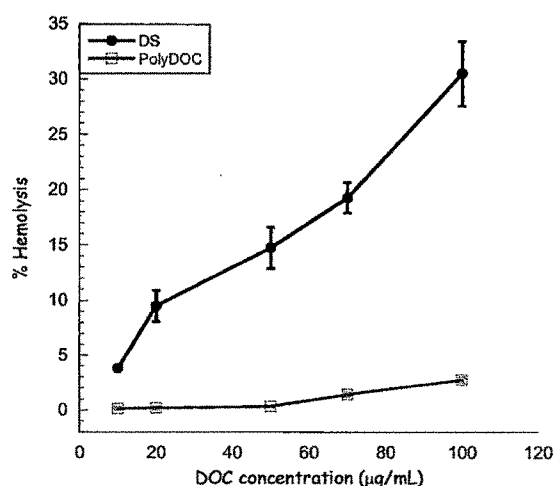


Figure 7.15 Hemolytic activities of the PolyDOC and DS. Each data was repeated three times to provide the standard deviation (n=3).

7.15.6. Biodistribution study of ^{99m}Tc -labelled compounds

Biodistribution pattern of ^{99m}Tc -PolyDOC and free ^{99m}Tc -DS were investigated in EAT bearing mice with 2mg/kg body weight dose equivalent to DOC. Figure 7.16 represents complete tissue distribution after intravenous administration of ^{99m}Tc -labeled compounds (PolyDOC and DS) and results expressed in ^{99m}Tc -labeled compounds (DS and PolyDOC) accumulated per gram of tissue (expressed as percentage of the injected dose/g tissue, %ID/g) at different time intervals. PolyDOC uptake in tissue was significant ($P < 0.01$) in each organs than DS.

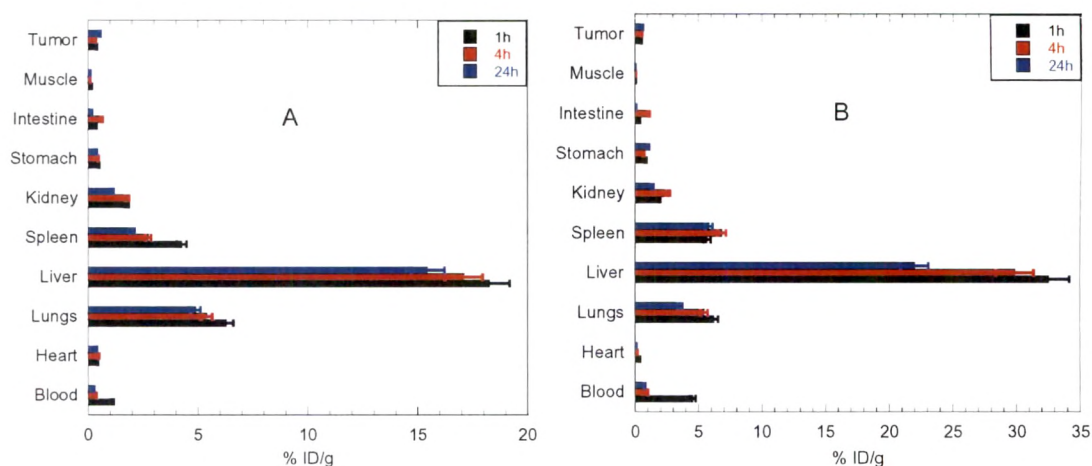


Figure 7.16 Tissue distributions of ^{99m}Tc -DS (A) and (B) for ^{99m}Tc -PolyDOC after intravenous injection in BalB/c mice at a single dose of 2 mg/kg. Each point represents the mean of three mice \pm S.D. ($n = 3$).

Results demonstrate that liver, lungs and spleen are the organs of preferential accumulation of ^{99m}Tc -PolyDOC. After 1h, 32.52 % \pm 2.91, 6.2 % \pm 0.47 and 5.68 % \pm 0.36 of the injected activity was accumulated in the liver, lungs and spleen, respectively. However, DS formulation uptake in tissue was also more after 1h in liver > lungs > spleen (18.2% \pm 1.31 > 6.3% \pm 0.48 > 4.26% \pm 0.27 respectively). PolyDOC uptake was significantly high ($P < 0.05$) in tumor compared to DS (Figure 7.17).

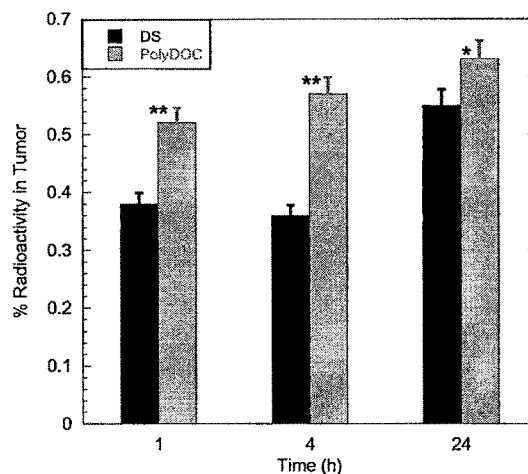


Figure 7.17 Tumor uptakes of ^{99m}Tc -DS and ^{99m}Tc -PolyDOC. Each point represents the mean of three mice \pm S.D. (* $P < 0.05$ vs. DS, ** $P < 0.001$ vs. DS).

Hyaluronan uptake in liver and spleen is mediated by presence of Hyaluronan Receptor for Endocytosis (HARE) and increases as molecular weight increase (Zhou et al., 2000; Sugahara et al., 2001; Harris et al., 2007). ^{99m}Tc labeled hyaluronan-paclitaxel bioconjugate (^{99m}Tc -ONCOFID-P) was approximately 80 % and 6 % of the injected activity was accumulated in the liver and spleen respectively (Meléndez-Alafort et al., 2006, Banzatoa et al., 2009). Therefore, above mentioned reason could be explanation of removal of PolyDOC by liver and spleen.

We had determined the liver/blood ratio of ^{99m}Tc -DC and ^{99m}Tc -PolyDOC and are shown in figure 7.18A. PolyDOC reduce significantly ($P < 0.01$) the ratio between liver/blood than DS which indicate PolyDOC clearance was delayed compared to free DS formulation after IV injection of PolyDOC. In addition, we also determined ratio of uptake of DS and PolyDOC between tumor and muscle (opposite side than tumor) (Figure 7.18B). Interestingly, PolyDOC showed high ratio of uptake between tumor and muscles and was significantly ($P < 0.001$) higher than DS.

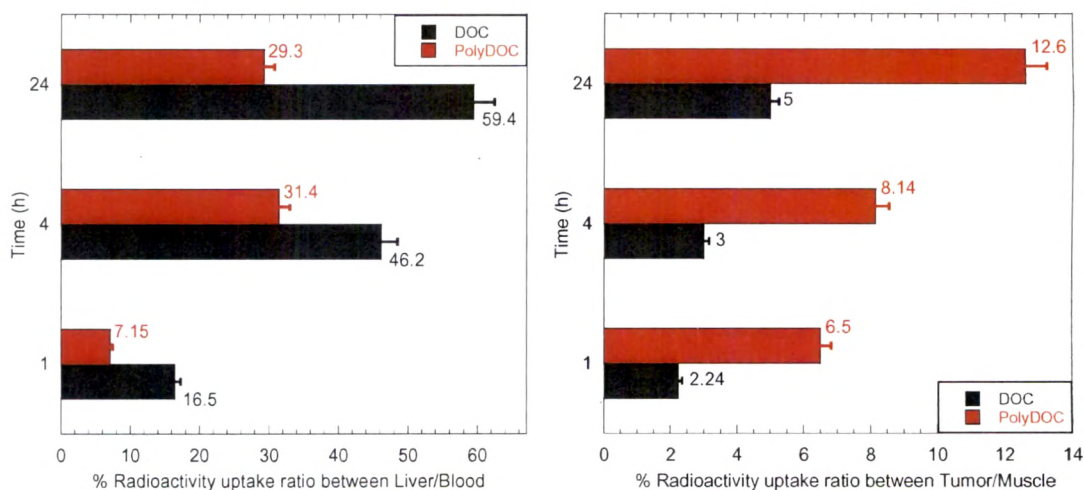


Figure 7.18 (A) Liver/Blood uptake ratio ($p < 0.01$, PolyDOC vs. DOC) and (B) Tumor/Muscle uptake ratio ($p < 0.001$, PolyDOC vs. DOC).

7.16. Conclusion

Docetaxel, a hydrophobic anticancer drug was successfully encapsulated in polymersomes by nanoprecipitation method and enable to release DOC in a control manner *in vitro* at pH 5.5 and 7.4 for 10 days. PolyDOC were stable at 4⁰C for 1 month and more than six month in form of lyophilized sample. PolyDOC was equipotent or more potent after 24h in both cells compare to free DOC and DS formulation. Due to difference in CD44 expression level in both cells, PolyDOC showed more cytotoxicity in MCF-7 cells than U87 cells at each time point. ^{99m}Tc labeling of DS formulation and PolyDOC were prepared by a direct method with more than 98% radiolabeling efficiency. Labeled compounds were stable *in vitro*, *in vivo* and against DTPA challenge. Blood circulation ($t_{1/2}$) and mean residence time (MRT) had increased for PolyDOC compared to DS. Biodistribution data demonstrated that PolyDOC were successfully accumulated at the tumor tissue owing to the passive accumulation (EPR effect) and active targeting (CD44 mediated endocytosis) in EAT bearing mice. PolyDOC uptake in tumor was more at each time point compare to DS. In addition, Tumor/Muscle uptake ratio of PolyDOC was high compare to DS formulation. PolyDOC could be efficient drug delivery carrier for improving docetaxel chemotherapy.

References

- Discher DE, Ahmed F. Polymersomes. *Annu Rev Biomed Eng* 2006;8:323-41.
- Upadhyay K, Agrawal H, Upadhyay C, Schatz C, Le Meins J, Misra A, Lecommandoux S. Role of block copolymer nanoconstructs in cancer therapy. *Crit Rev Ther Drug Carrier Syst* 2009;26(2):157-205.
- Guéritte-Voegelein F, Guénard D, Lavelle F, Le Goff M-T, Mangatal L, Potier P. Relationships between the structure of taxol analogues and their antimitotic activity. *Journal of Medicinal Chemistry* 1991;34(3):992-8.
- Clarke SJ, Rivory LP. Clinical pharmacokinetics of docetaxel. *Clin Pharmacokinet* 1999;36(2):99-114.
- ten Tije AJ, Verweij J, Loos WJ, Sparreboom A. Pharmacological effects of formulation vehicles: implications for cancer chemotherapy. *Clin Pharmacokinet* 2003;42(7):665-85.
- Esmaeili F, Dinarvand R, Ghahremani MH, Amini M, Rouhani H, Sepehri N, Ostad SN, Atyabi F. Docetaxel-albumin conjugates: preparation, in vitro evaluation and biodistribution studies. *J Pharm Sci* 2009;98(8):2718-30.
- Esmaeili F, Ghahremani MH, Ostad SN, Atyabi F, Seyedabadi M, Malekshahi MR, Amini M, Dinarvand R. Folate-receptor-targeted delivery of docetaxel nanoparticles prepared by PLGA-PEG-folate conjugate. *J Drug Target* 2008;16(5):415-23.
- Xie Z, Lu T, Chen X, Zheng Y, Jing X. Synthesis, self-assembly in water, and cytotoxicity of MPEG-block-PLLA/DX conjugates. *J Biomed Mater Res A* 2009;88(1):238-45.
- Feng SS, Mei L, Anitha P, Gan CW, Zhou W. Poly(lactide)-vitamin E derivative/montmorillonite nanoparticle formulations for the oral delivery of Docetaxel. *Biomaterials* 2009;30(19):3297-306.

- Chan JM, Zhang L, Yuet KP, Liao G, Rhee JW, Langer R, Farokhzad OC. PLGA-lecithin-PEG core-shell nanoparticles for controlled drug delivery. *Biomaterials* 2009;30(8):1627-34.
- Xu Z, Chen L, Gu W, Gao Y, Lin L, Zhang Z, Xi Y, Li Y. The performance of docetaxel-loaded solid lipid nanoparticles targeted to hepatocellular carcinoma. *Biomaterials* 2009;30(2):226-32.
- Immordino ML, Brusa P, Arpicco S, Stella B, Dosio F, Cattel L. Preparation, characterization, cytotoxicity and pharmacokinetics of liposomes containing docetaxel. *J Control Release* 2003;91(3):417-29.
- Hwang HY, Kim IS, Kwon IC, Kim YH. Tumor targetability and antitumor effect of docetaxel-loaded hydrophobically modified glycol chitosan nanoparticles. *J Control Release* 2008;128(1):23-31.
- Elsabahy M, Perron ME, Bertrand N, Yu GE, Leroux JC. Solubilization of docetaxel in poly(ethylene oxide)-block-poly(butylene/styrene oxide) micelles. *Biomacromolecules* 2007;8(7):2250-7.
- Liu B, Yang M, Li R, Ding Y, Qian X, Yu L, Jiang X. The antitumor effect of novel docetaxel-loaded thermosensitive micelles. *Eur J Pharm Biopharm* 2008;69(2):527-34.
- Du W, Hong L, Yao T, Yang X, He Q, Yang B, Hu Y. Synthesis and evaluation of water-soluble docetaxel prodrugs-docetaxel esters of malic acid. *Bioorg Med Chem* 2007;15(18):6323-30.
- Huynh L, Leroux JC, Allen C. Enhancement of docetaxel solubility via conjugation of formulation-compatible moieties. *Org Biomol Chem* 2009;7(17):3437-46.
- Liu S, Edwards DS, Barrett JA. ^{99m}Tc labeling of highly potent small peptides. *Bioconjug Chem* 1997;8(5):621-36.
- Meléndez-Alafort L, Riondato M, Nadali A, Banzato A, Camporese D, Boccaccio P, Uzunov N, Rosato A, Mazzi U. Bioavailability of ^{99m}Tc-Ha-paclitaxel

complex [^{99m}Tc -ONCOFID-P] in mice using four different administration routes. *Journal of Labelled Compounds and Radiopharmaceuticals* 2006;49(11):939-50.

- Harivardhan Reddy L, Sharma RK, Chuttani K, Mishra AK, Murthy RS. Influence of administration route on tumor uptake and biodistribution of etoposide loaded solid lipid nanoparticles in Dalton's lymphoma tumor bearing mice. *J Control Release* 2005;105(3):185-98.
- Vaishampayan U, Parchment RE, Jasti BR, Hussain M. Taxanes: an overview of the pharmacokinetics and pharmacodynamics. *Urology* 1999;54(6A Suppl):22-9.
- Gao Y, Chen L, Gu W, Xi Y, Lin L, Li Y. Targeted nanoassembly loaded with docetaxel improves intracellular drug delivery and efficacy in murine breast cancer model. *Mol Pharm* 2008;5(6):1044-54.
- Quaglia F, Ostacolo L, Mazzaglia A, Villari V, Zaccaria D, Sciortino MT. The intracellular effects of non-ionic amphiphilic cyclodextrin nanoparticles in the delivery of anticancer drugs. *Biomaterials* 2009;30(3):374-82.
- Saha GB. *Fundamentals of Nuclear Pharmacy*. Fifth Edition. 2004. Springer-Verlag New York, Inc., US.
- Panwar P, Singh S, Kumar N, Rawat H, Mishra AK. Synthesis, characterization, and in vivo skeletal localization of a new ^{99m}Tc -based multidentate phosphonate chelate: 5-Amino-1,3-bis(ethylamine-(N,N dimethyl diphosphonic acid) acetamido) benzene. *Bioorganic and Medicinal Chemistry* 2007;15(2):1138-45.
- Cheon Lee S, Kim C, Chan Kwon I, Chung H, Young Jeong S. Polymeric micelles of poly(2-ethyl-2-oxazoline)-block-poly(epsilon-caprolactone) copolymer as a carrier for paclitaxel. *J Control Release* 2003;89(3):437-46.
- Mishra AK, Iznaga-Escobar N, Figueredo R, Jain VK, Dwarakanath BS, Pérez-Rodríguez R, Sharma RK, Mathew TL. Preparation and comparative evaluation of ^{99m}Tc -labeled 2-iminothiolane modified antibodies and CITC-DTPA

- immunoconjugates of anti-EGF-receptor antibodies. *Methods Find Exp Clin Pharmacol* 2002; 24(10):653-60.
- Wu MS, Robbins JC, Bugianesi RL, Ponpipom MM, Shen TY. Modified in vivo behavior of liposomes containing synthetic glycolipids. *Biochim Biophys Acta* 1981;674(1):19-29.
 - Arulsudar N, Subramanian N, Mishra P, Chuttani K, Sharma RK, Murthy RS. Preparation, characterization, and biodistribution study of technetium-99m-labeled leuprolide acetate-loaded liposomes in ehrlich ascites tumor-bearing mice. *AAPS J* 2004;6(1):45-56.
 - Agashe HB, Babbar AK, Jain S, Sharma RK, Mishra AK, Asthana A, Garg M, Dutta T, Jain NK. Investigations on biodistribution of technetium-99m-labeled carbohydrate-coated poly(propylene imine) dendrimers. *Nanomedicine* 2007;3(2):120-7.
 - Shuai X, Ai H, Nasongkla N, Kim S, Gao J. Micellar carriers based on block copolymers of poly(epsilon-caprolactone) and poly(ethylene glycol) for doxorubicin delivery. *J Control Release* 2004;98(3):415-26.
 - Peer D, Margalit R. Tumor-targeted hyaluronan nanoliposomes increase the antitumor activity of liposomal Doxorubicin in syngeneic and human xenograft mouse tumor models. *Neoplasia* 2004;6(4):343-53.
 - Banzato A, Rondina M, Meléndez-Alafort L, Zangoni E, Nadali A, Renier D, Moschini G, Mazzi U, Zanovello P, Rosato A. Biodistribution imaging of a paclitaxel-hyaluronan bioconjugate. *Nucl Med Biol* 2009;36(5):525-33.
 - Rittierodt M, Harada K. Repetitive doxorubicin treatment of glioblastoma enhances the PGP expression--a special role for endothelial cells. *Exp Toxicol Pathol* 2003;55(1):39-44.